IIETA International Information and Engineering Technology Association
Advancing the World of Information and Engineering

Revue des Composites et des Matériaux Avancés-Journal of Composite and Advanced Materials
Vol. 31, No. 4, August, 2021, pp. 249-255
Journal homepage: http://iieta.org/journals/rcma

The Electromagnetic Wave Absorption Performance and Mechanical Properties of Cement-Based Composite Material Mixed with Functional Aggregates with High Fe_2O_3 and SiC

Zuoqun Zhang*, Chaoshan Yang, Hua Cheng, Xiaohan Huang, Yuhao Zhu

Department of Civil Engineering, Army Logistics University of PLA, Chongqing 401311, China

Corresponding Author Email: ZZQDLSF@163.com

https://doi.org/10.18280/rcma.310409

Received: 3 April 2021
Accepted: 8 July 2021

Keywords:
cement-based electromagnetic wave absorbing material, wave absorbing agent, mechanical properties

ABSTRACT

Now there're many researches on the electromagnetic radiation protection function of the cement-based electromagnetic wave absorbing materials, such materials have been widely used in various types of buildings. This paper proposed an idea for preparing a cement-based composite material by mixing functional aggregates with high content of Fe_2O_3 and SiC, that is, adding Fe_3O_4 powder and nano-SiC of different contents in the clay, and then sintering at 1190°C; the prepared aggregates showed obvious magnetic loss and dielectric loss to electromagnetic waves, and the numerical tube pressure could reach 16.83MPa. The double-layer reflectivity test board made of functional aggregates showed excellent electromagnetic wave absorption performance, its reflection loss was less than -10dB in the frequency range of 8~18GHz (corresponding to energy absorption greater than 90% EM), and its maximum RL reached -12.13dB. In addition, the compressive strength of the cement-based composite material at the age of 28 days reached 50.1 MPa, which can meet the strength requirements of building materials.

1. INTRODUCTION

Accompanying the advancement of electronic technology, electromagnetic radiation is generated in great amount and considered to be the fourth type of pollution source. Electromagnetic radiation can damage human body, causing thermal effect, hysteresis effect, and cumulative effect, etc., moreover, the leakage of political, economic, and military information caused by electromagnetic radiation will seriously endanger the security of a country [1, 2]. There are two ways to reduce electromagnetic radiation: absorption and reflection. However, the reflection method can only change the propagation direction of electromagnetic waves, it cannot consume the electromagnetic waves or truly reduce the harm of electromagnetic radiation, therefore, as important materials that can reduce the harm of electromagnetic waves, the wave-absorbing materials have been used extensively in civil and military buildings, and the cement-based material is the one with the greatest usage amount and the widest application range; by incorporating electromagnetic wave absorbent and designing multiple layers or new surface layer structure, we can improve the electromagnetic wave absorption performance of the material [3-6]. Dai et al. [7] fabricated a cement-based composite material with broadband absorption and high strength by mixing carbon black with different contents. Wang et al. [8] mixed coiled carbon fiber into cement base to prepare a wave-absorbing material. Guo [9] prepared a carbon nanotubes suspension using a surfactant ultrasonic treatment method, he mixed multi-walled carbon nanotubes into the cement base to produce a composite material and studied its mechanical properties and wave absorption performance. Guo et al. [10] used natural magnetite powder to prepare a cement-based absorbing composite material. He et al. [11] and Nan et al. [12] incorporated iron tailings into the cement base to prepare a magnesium oxysulfate foam cement-based composite material. Dai et al. [13, 14] studied the wave absorption performance of a special-shaped steel fiber cement-based material. Literatures [15-17] reported the influence of different kinds of nanomaterials mixed into cement base on the absorption of electromagnetic waves. Literatures [18-22] reported a few researches on cement-based electromagnetic wave absorbing materials mixed with composite wave absorbing agents. However, in these studies, the volume of aggregates accounted for about 60% of the cement-based material, aggregates such as crushed stone have a weak ability to absorb electromagnetic waves, and the incorporation of wave absorbing agent in the cement paste will affect the overall mechanical properties of the material. Therefore, in order to make full use of the aggregates that account for a large proportion in the cement-based material, this paper proposed to prepare the functional aggregates by mixing clay, Fe_3O_4 powder, and nano-SiC, and sintering at a high temperature. Then, this paper studied the phase composition, micro morphology of its outside and inside, electromagnetic parameters, and numerical tube pressure of the prepared aggregates, and the reflection loss and compressive strength of the double-layer test boards made of the different functional aggregates.

2. ABOUT THE EXPERIMENT

2.1 Raw materials

In the experiment, the clay powder produced by Changzhou Dingbang Mineral Products Technology Co., Ltd. was taken

as the host material of the functional aggregates, Table 1 below lists the content of each kind of oxide in the clay. The Fe_3O_4 content was between 5.7% and 6.7%, which had a positive effect on the electromagnetic wave loss of the aggregates. 38μm Fe_3O_4 (purity 99.99%) produced by Hebei Hangbei Metal Material Co., Ltd. and SiC (purity 99.9%, average particle size 500nm) produced by Taipeng Metal Material Co., Ltd. were taken as the precursors of the absorption phase. The cement used to prepare the composite material was P.O 42.5 Portland cement (according to Chinese Standard GB 175-2007). Fly ash produced by Henan Boruntao Material Co., Ltd. was taken as the admixture of the cement-based material, besides reducing costs, it could also improve the material's resistance to sulfate and chemical attack. The particle size of fly ash was relatively small, which was good for improving the overall particle size distribution and increase the strength of the material. Quartz sand with a fineness modulus of 2.9 was taken as the fine aggregate to prepare the cement-based material. Expanded perlite with an apparent density of 120kg/m^3 and an average diameter of 1.1mm was taken as the material of the matching layer.

Table 1. Content of each oxide in clay (wt.%)

Composition	SiO_2	Al_2O_3	Fe_2O_3	Na_2O	K_2O	CaO	MgO	MnO	TiO_2	Ignition loss
Content	55.6-60.5	9.0-10.1	5.7-6.7	0.03-0.11	0.96-1.30	0.42-1.95	10.7-11.35	0.61	0.32-0.63	10.53-11.80

2.2 Experimental process

According to the mass fraction ratios listed in Table 2, clay powder, Fe_3O_4, and nano-SiC were mixed in a drum-type ball mill tank for 15 minutes, each time, 2.4kg of the raw materials was mixed, the mixing time was 3h, and the rotation speed was 200r/min. Then, 40wt% water was added to the powder mixer and mixed in the shear mixer for 8 minutes. After that, the paste was added into the rotary granulator in batches to produce granules with a particle size of 9-12 mm, which were then dried at 105℃ for 8h, sintered in a high-temperature resistance furnace at a rate of 5℃·min^{-1}, kept at 600℃ for 8min, then heated to 1190℃ and kept for 60min. At last, the aggregates were cooled to 130℃ in the furnace at a rate of 6℃·min^{-1}, and then taken out and naturally cooled to room temperature, in this way, the functional aggregates that can absorb the electromagnetic waves were prepared.

Table 2. Ratio of raw materials of the functional aggregates

Serial No.	Nano-SiC content (wt.%)	Fe_3O_4 content (wt.%)	Clay powder content (wt.%)	Maximum sintering temperature (℃)
S1	10	0	100	1190
SF2	10	20	70	1190
SF3	5	10	85	1190
SF4	10	10	80	1190
SF5	5	10	85	1150
SF6	5	10	85	1110
F7	0	10	90	1190
N8	0	0	100	1190

The prepared functional aggregates were used to prepare the wave absorbing layer of the cement-based composite material. At first, the cement, sand, fly ash, and water were mixed for 1 min at a mass ratio of 1:1.1:0.1:0.32. Then, the pre-wetted aggregates with a dry surface were added into the paste and mixed for 2min, the volume ratio of the cement slurry and the ceramsite aggregate was controlled at 55%:45%. After fully mixed, the mixture was poured into a mold with a size of 180mm×180mm×40mm until a height of 30mm, and vibrated on a vibrator for 1 min. After 1h, a 10mm thick matching layer was added on top of the newly cast wave absorbing layer; the matching layer was a layer of mortar, the volume ratio of expanded perlite to cement slurry was 60%:40%, and the mass ratio of water to cement was 0.32. Then, with this prepared cement-based composite material, several test pieces of a size of 150mm×150mm×150mm were fabricated for the compressive strength test. All test pieces were cured in a standard curing room for 24h, removed from the mold, and put into a standard curing room for curing. The temperature of the curing room was 20℃±2℃, and the relative humidity was above 95%.

Also, test pieces of cement-based materials made of ordinary ceramsite and crushed stone aggregates were prepared and taken as the control group, their content ratio was the same as that of the proposed composite material, also a same 10mm thick matching layer was added on the top; the particle size range of the crushed stone was 8-12mm, and the particle size of ceramsite granules was about 10mm. The preparation process of the ordinary ceramsite aggregate was the same as that of the proposed functional aggregate except that no Fe_3O_4 or nano-SiC was added.

2.3 Test methods

X-ray (XRD) was used to examine the mineral phases of the clay powder, the functional aggregates, and the cement. The model DX-2700 X-ray diffractometer used in the test was produced by the Dandong Haoyuan Instrument Co., Ltd. The functional aggregates were ground and then finely ground for the test, the scanning range was 15°~65° (2θ), and the MDI Jade software was used to process and analyze the data. Also, the model Quanta TM 250FEG field emission scanning electron microscope (SEM) produced by American company FEI was used to obtain the SEM images.

SEM uses a focused and narrow high-energy electron beam to scan the samples, through the interaction between the beam and the substance, different physical information could be triggered, then, by collecting, amplifying, and re-imaging the information, it could achieve the purpose of characterizing the microstructure of the substance. In the test, SEM was used to scan the surface and cross-section of the functional aggregate to observe its surface and internal structure after sintering. Aggregates of different proportions were mixed with water and fabricated into rectangular-shaped test pieces, which were sintered under the same conditions, after cooling, a model 3L SERIES V800 machine tool was used to polish the test pieces into standard sizes for rectangular waveguide test. Standard sizes for the rectangular waveguide test were: 22.86×10.16×2.5mm for 8-12GHz band, and 15.8×7.9×2.5mm for 12-18GHz band; then, their complex permeability and complex permittivity were measured and calculated on vector network analyzer (model: Keysight

N5227B). The reflectivity of the cement-based composite material test board was measured in a dark room using the arch method. The numerical tube pressure of the functional aggregates and the compressive strength of the cement-based composite material were tested on an MTS-2000 test system.

3. EXPERIMENTAL RESULTS AND ANALYSIS

3.1 Phase composition of the functional aggregates

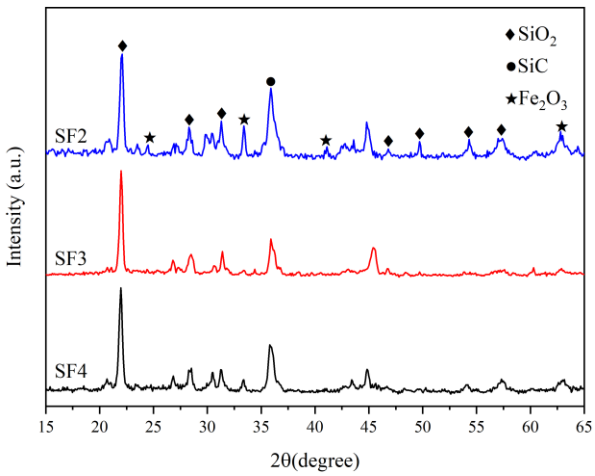

Figure 1. XRD spectrum of functional aggregates

The XRD spectrum of aggregates made of different raw materials is shown in Figure 1, strong and sharp peaks can be observed in the figure, and analysis showed that the main crystal phases of the aggregates after sintering were Fe_2O_3, SiO_2 and SiC. In the aggregates, the magnetic α-Fe_2O_3 and β-Fe_2O_3 produced by the oxidation of Fe_3O_4 play an important role in the absorption of electromagnetic waves. With the increase of Fe_2O_3 and SiC content, the characteristic peaks of Fe_2O_3 and SiC were enhanced while no new characteristic peak had appeared, indicating that no new substance was generated, and the composition of the functional aggregates after sintering was relatively stable.

3.2 Microstructure of the functional aggregates

Figure 2(a) is a SEM image of the surface of the functional aggregates, after high-temperature sintering, the surface of the functional aggregates was glazed and became smoother. Figures 2(b) and 2(c) are the SEM images of the cross-section of the functional aggregates, after sintering, there're a lot of closed pores and some connected pores in the aggregates, which were generated due to the decomposition of sulfate, carbonate, and other substances in the clay powder under high temperature. The generation of these pores enhanced the electromagnetic wave resonance loss of the functional aggregates and improved their wave absorption performance. In Figure 2(d), we can see that a large number of SiC and Fe_2O_3 granules (bright white particles) were embedded and evenly distributed inside the aggregates, so the wave absorption performance of the functional aggregates could be guaranteed.

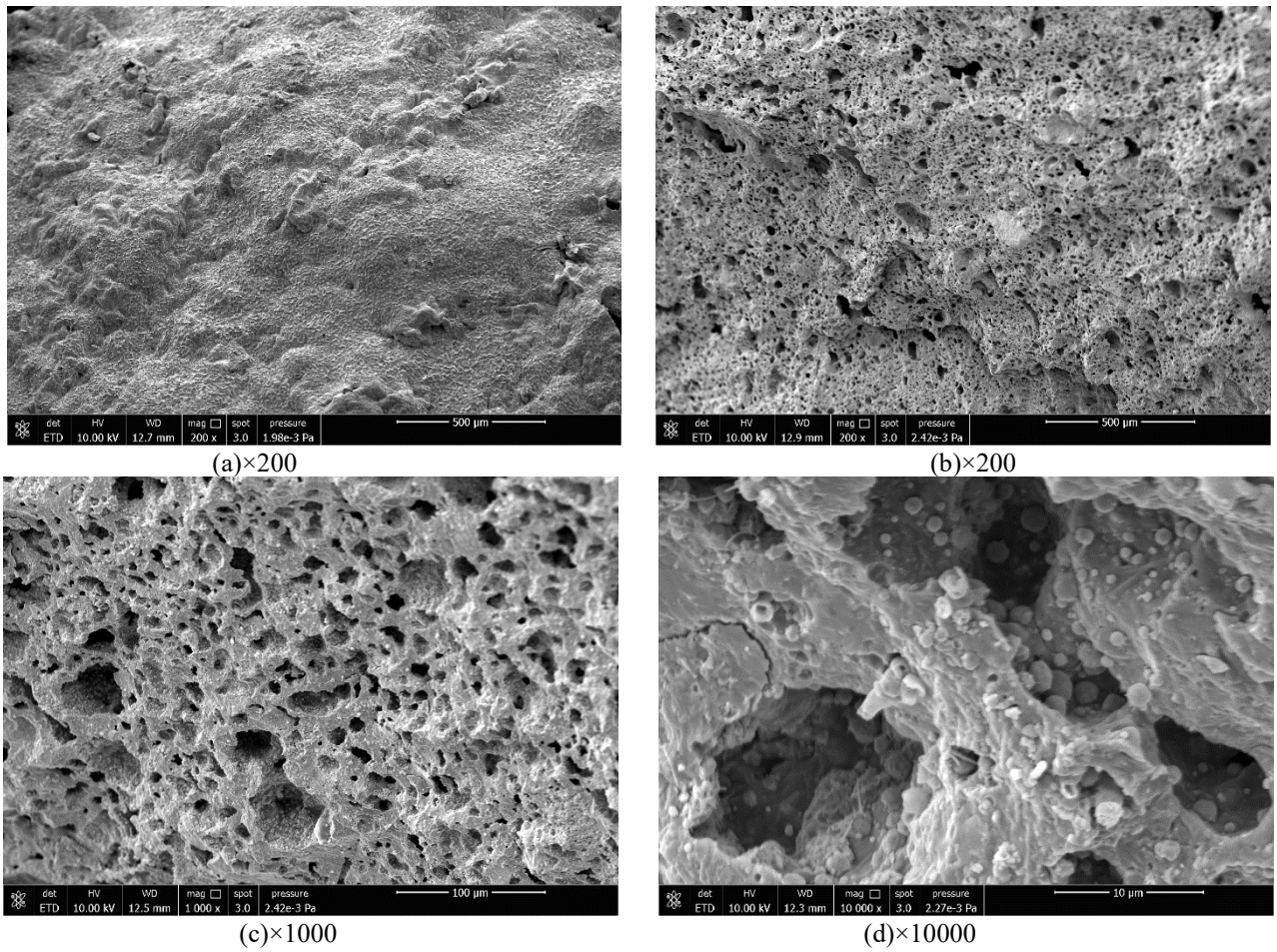

(a)×200 (b)×200

(c)×1000 (d)×10000

Figure 2. SEM images of functional aggregates (a is the surface; b, c, d are the inside)

3.3 Electromagnetic parameters of the functional aggregates

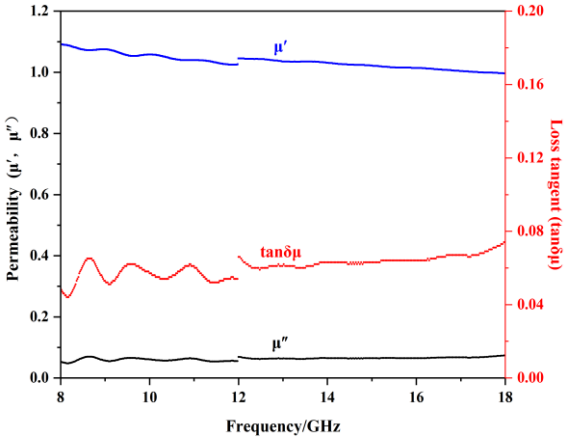

(a) SF2 permeability

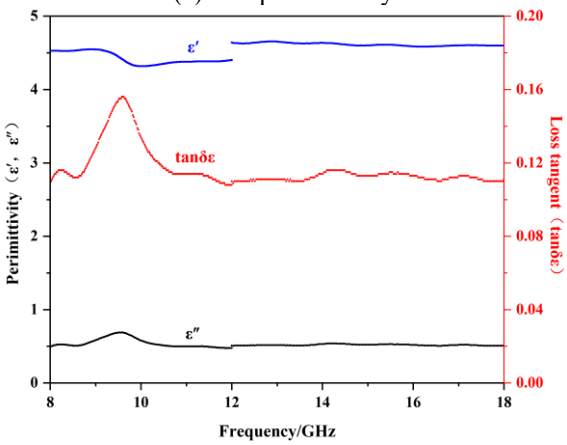

(b) SF2 permittivity

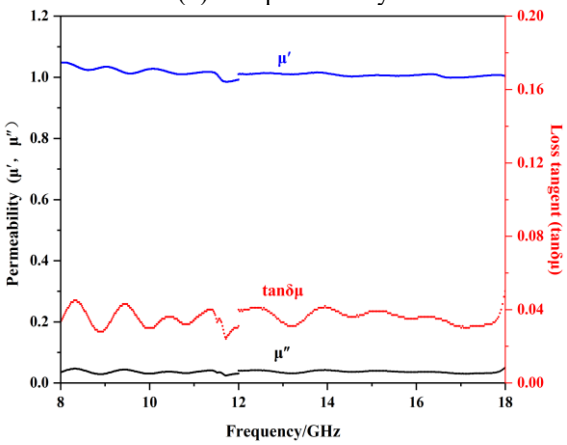

(c) SF3 permeability

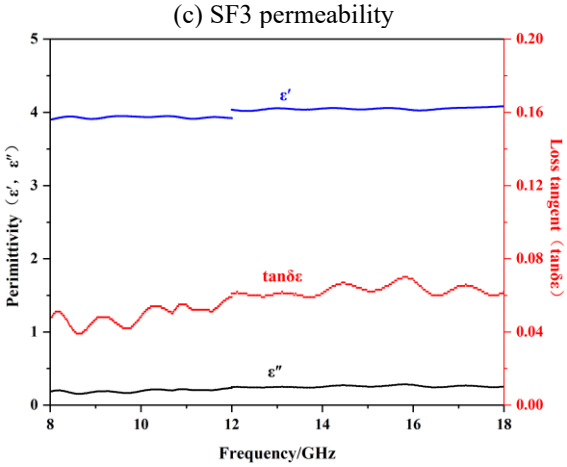

(d) SF3 permittivity

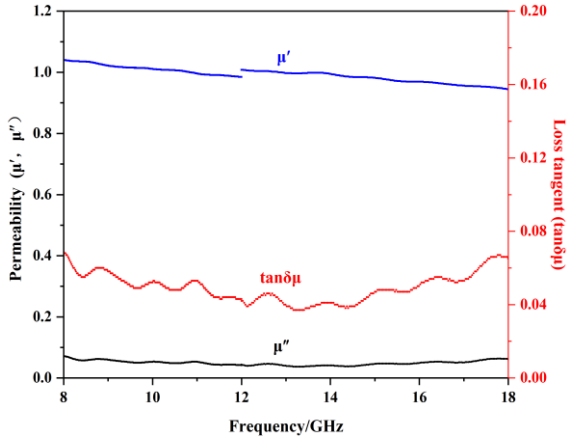

(e) SF4 permeability

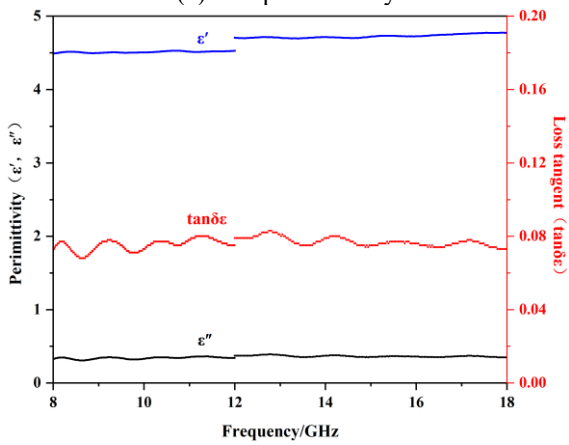

(f) SF4 permittivity

Figure 3. Electromagnetic parameters of different functional aggregates

According to the theory of electromagnetism, the imaginary part of the electromagnetic parameters of the material and the tangent angle of the loss are the main factors determining the characteristics of the electromagnetic loss of the material. By testing the electromagnetic parameters of different functional aggregates, analyzing the corresponding laws, and adjusting the composition of the aggregates, we could realize the purpose of adjusting the impedance matching and improving the overall wave-absorbing ability of the material. According to Figure 3, in the test frequency band of 8-18GHz, the real part μ' of the magnetic permeability of the SF2 aggregate was between 1-1.09, and the imaginary part μ'' was between 0.048-0.074. The tangent angle of magnetic permeability $tan\delta\mu$ was the ratio of μ'' to μ' [23], and its value was between 0.05 and 0.07. The real part ε' of its permittivity was between 4.32-4.65, the imaginary part ε'' was between 0.493-0.689, and the $tan\delta\varepsilon$ was between 0.11-0.16. The imaginary part of the electromagnetic parameters of the material and the tangent angle of the loss were relatively large, the aggregates showed a good magnetic loss effect, which was related to the wave absorbing agents SiC and Fe_3O_4. The real part of the permittivity ε' of SF3 aggregate was between 3.9-4.08, the imaginary part ε'' of the permittivity was between 0.153-0.283, and the tangent angle of the permittivity $tan\delta\varepsilon$ was between 0.04-0.07. The real part of the permittivity ε' was between 4.49-4.77, the imaginary part of the permittivity ε'' was between 0.306-0.391, and the tangent angle of the permittivity $tan\delta\varepsilon$ was between 0.07-0.08. By comparing the values of the imaginary part of the electromagnetic parameters and the tangent angle of the permittivity of the three groups of

functional aggregates, it could be seen that when the SiC content was between 5%-10% and the Fe_3O_4 content was between 10%-20%, with the increase of the SiC and Fe_3O_4 content, the electromagnetic loss effect of the functional aggregates got better, and the electromagnetic loss effect of the SF2 aggregate was the best.

3.4 Numerical tube pressure of the functional aggregates

The functional aggregate accounted for 45% of the total volume of the cement-based composite material. The numerical tube pressure of the aggregate has a direct impact on the mechanical properties of the cement-based material. Through the test on the numerical tube pressure of the aggregates, this study explored the impact of different sintering temperatures and raw material contents on the strength of the aggregates, the sintering conditions previously obtained through multiple tests were given in Section 2.2, and Figure 4 shows the test data of the numerical tube pressure of different aggregates. Through the test data of SF3, SF5 and SF6, we can see that the numerical tube pressure of the aggregates increased with the rise of sintering temperature, at about 1190℃, the surface of the aggregate was glazed obviously, which was beneficial to improving the numerical tube pressure. According to the test data of SF2, SF3, SF4, and N8, it can be concluded that the numerical tube pressure increased with the increase of SiC and Fe_3O_4 content, this is because the strength of SiC is relatively large, when the SiC and Fe_3O_4 content increases, the content of SiO_2 decreases, and the bulk density of the aggregate increases accordingly, factors such as the change of porosity do not have much impact on the numerical tube pressure of the aggregate.

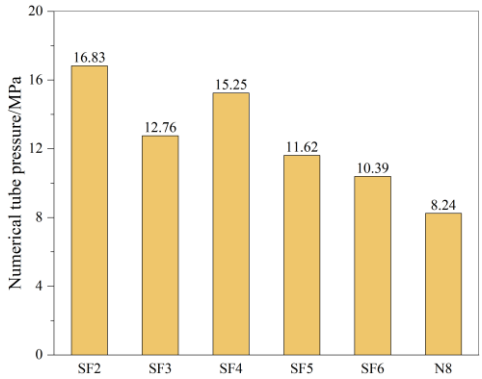

Figure 4. Numerical tube pressure of different aggregates

3.5 Wave absorption performance of the cement-based composite material

Design of the test boards made of the cement-based composite material is shown in Table 3, and the reflection loss values of the test boards are given in Figure 5(a)-(d). The wave absorption performance can be described by the reflection loss, under the same test conditions, a smaller value of reflection loss indicates that the material has a stronger ability to weaken the electromagnetic wave loss, and it means that the material has a better wave absorption performance. Figure 5(a) shows that in the 8-18GHz frequency range, the reflection loss of ordinary crushed stone concrete test piece T7 was between -3.81dB and -5.35dB, and the reflection loss of ordinary clay ceramsite test piece T8 was between -5.28dB and -6.47dB, indicating that the electromagnetic wave absorption performance of the ceramsite-containing material was better than that of ordinary crushed stone concrete. Inside the ordinary clay ceramsite, the resonant cavities formed by the porous structure can absorb electromagnetic waves through the resonance absorption effect [24], but the two test boards showed low absorption of electromagnetic waves, both cannot meet the civil application requirement (-7dB) for electromagnetic wave absorption. According to Figure 5(b), the reflection loss values of the single-layer and double-layer test pieces T5 and T6 made of the F7 aggregate were -6.16~-8.35dB and -7.26~-9.01dB, respectively. The electromagnetic wave absorption performance of the double-layer test piece had been improved significantly. Related studies suggest that, adding porous materials with lower electromagnetic parameters can effectively reduce the permittivity of the composite material, and the addition of a matching layer can increase the amount of incident electromagnetic waves. Expanded perlite is a high-porosity wave-transmitting material with low electromagnetic parameters, the many pores form a honeycomb shaped-structure inside the material; the matching layer made of this material can decrease the impedance difference between the air and the test board, and reduce interface reflection, thereby improving the impedance matching performance of the test board, which is conducive to the absorption of electromagnetic waves by the absorbing layer. According to Figure 5(c), the reflection loss of the T3 test piece in the 8-18GHz frequency band was -8.71~-9.77dB, and the reflection loss of the T4 test piece was -9.02~-11.13dB. Test results showed that the T3 test piece had the best wave absorption performance. For the cement-based composite material, when the content of functional aggregate and the content of Fe_3O_4 in the aggregate were kept the same, and the content of nano-SiC in the aggregate was within the range of 0~10 wt.%, the wave absorption ability of the test boards enhanced with the increase of the content of SiC. According to Figure 5(d), the reflectivity of the T1 test piece was -8.52~-8.97dB, the reflectivity of the T2 test piece was -10.14~-12.13dB, when the content of aggregate and the content of nano-SiC in the aggregate were kept the same, and the content of 38μm Fe_3O_4 in the aggregate was within the range of 0-20%, the wave absorption ability of the test boards enhanced with the increase of the content of 38μm Fe_3O_4.

Table 3. Test boards made of the cement-based composite material

Serial number of the test board	Type of aggregate	10mm thick matching layer	Total thickness (mm)
T1	S1	Yes	40
T2	SF2	Yes	40
T3	SF3	Yes	40
T4	SF4	Yes	40
T5	F7	No	30
T6	F7	Yes	40
T7	Crushed stone	Yes	40
T8	N8	Yes	40

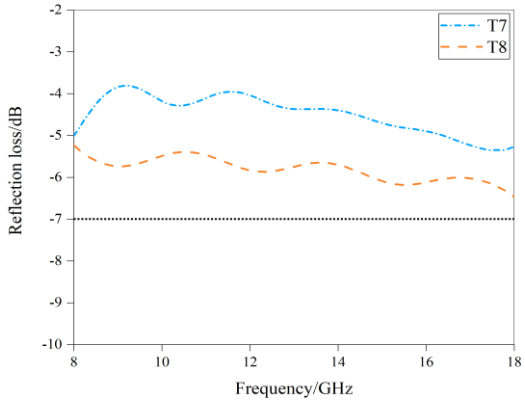

(a) Reflection loss of test pieces mixed with crushed stone and ordinary ceramsite aggregates

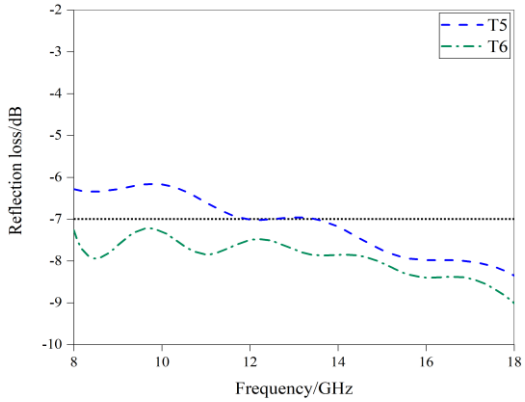

(b) Reflection loss of single-layer and double-layer test pieces

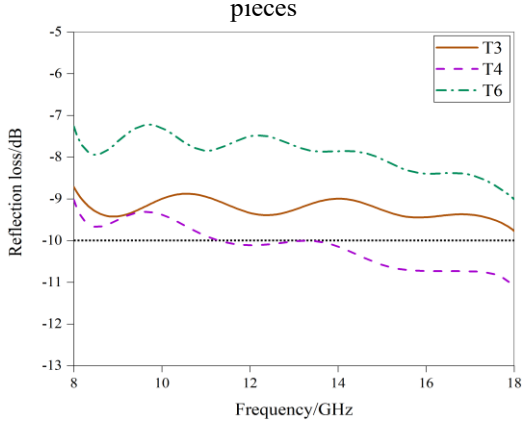

(c) Reflection loss of test pieces mixed with different contents of nano-SiC

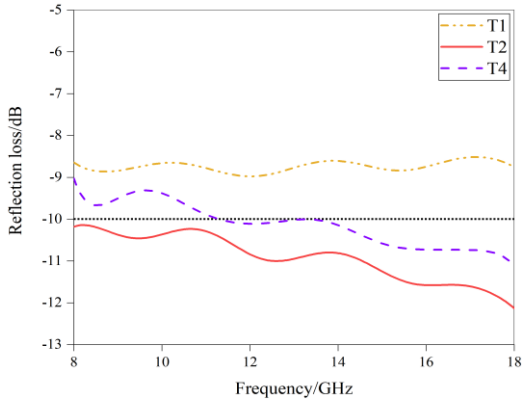

(d) Reflection loss of test pieces mixed with different contents of Fe_3O_4

Figure 5. Reflection loss of test pieces

3.6 Mechanical properties of the cement-based composite material

Under the same mixing ratio and curing conditions, the test data of the compressive strength of the wave-absorbing layer of the cement-based composite material containing different types of aggregates are shown in Figure 6. According to the figure, for the cement-based composite materials respectively containing SF2, SF3 and SF4 aggregates, their compressive strength values on the 28d were T2>T4>T3=45.2MPa, test pieces made of the functional aggregates generally had a high compressive strength. In early stage, the impact of different aggregates on the strength of the composite material was little, this is because the cement-base material had not completely hydrated in the early stage, so few gel material had been produced; then as the curing time increased, the bonding strength of the hydration product increased, the functional aggregates were wrapped, and the compressive strength of the material enhanced. According to the data of the 28d compressive strength of T2, T3, T4 test pieces we can see that, the compressive strength of the composite material was mainly affected by the strength of the functional aggregate, and the compressive strength increased with the increase of the numerical tube pressure. The T2 test piece prepared with the sintered high-strength aggregate had a 28d compressive strength as high as 50.1MPa, which showed excellent mechanical properties.

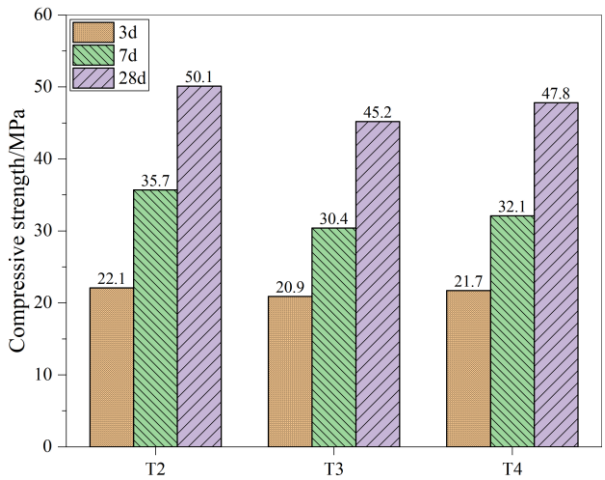

Figure 6. Compressive strength of test pieces containing different types of aggregates

4. CONCLUSION

In summary, this study fabricated functional aggregates with a porous internal structure by incorporating 38μm Fe_3O_4 and nano-SiC into clay and sintering at 1190°C. Test results of numerical tube pressure showed that, the strength of the SF2 aggregate mixed with 10wt.% nano-SiC and 20wt.% 38μm Fe_3O_4 reached 16.83MPa. Test results of the electromagnetic parameters suggested that the prepared aggregates had good magnetic loss and dielectric loss performance for electromagnetic waves. For the double-layer reflectivity test board T2 made of functional aggregate, under the joint action of the internal porous structure of the functional aggregate and the matching layer, the reflectivity in the 8-18GHz frequency range was less than -10dB (corresponding to energy absorption greater than 90% EM), and its maximum RL

reached -12.13dB, showing excellent electromagnetic wave absorption performance. In addition, the compressive strength of the cement-based composite material made of the functional aggregate reached 50.1 MPa at the age of 28 days, which can meet the strength requirements of building materials.

ACKNOWLEDGMENT

Funded by the Chongqing Postgraduate Research and Innovation Project (NB. CYS21530).

REFERENCES

[1] Cheng, K.B., Ramakrishna, S., Lee, K.C. (2000). Electromagnetic shielding effectiveness of copper/glass fiber knitted fabric reinforced polypropylene composites. Composites Part A: Applied Science and Manufacturing, 31(10): 1039-1045. https://doi.org/10.1016/S1359-835X(00)00071-3

[2] Sher, L. (2000). The effects of natural and man-made electromagnetic fields on mood and behavior: The role of sleep disturbances. Medical hypotheses, 54(4): 630-633. https://doi.org/10.1054/mehy.1999.0912

[3] Wang, Q., Zhang, X., Mao, Q., Ge, K., Zhou, M. (2002). Preparation of modified textile possessed of absorbing and shielding characterizations. In 2002 3rd International Symposium on Electromagnetic Compatibility, pp. 589-594. https://doi.org/10.1109/ELMAGC.2002.1177501

[4] Wu, J., Chung, D.D.L. (2002). Increasing the electromagnetic interference shielding effectiveness of carbon fiber polymer–matrix composite by using activated carbon fibers. Carbon, 40(3): 445-447. https://doi.org/10.1016/S0008-6223(01)00133-6

[5] Dai, Y., Sun, M., Liu, C., Li, Z. (2010). Electromagnetic wave absorbing characteristics of carbon black cement-based composites. Cement and Concrete Composites, 32(7): 508-513. https://doi.org/10.1016/j.cemconcomp.2010.03.009

[6] Guan, H., Liu, S., Duan, Y., Cheng, J. (2006). Cement based electromagnetic shielding and absorbing building materials. Cement and Concrete Composites, 28(5): 468-474. https://doi.org/10.1016/j.cemconcomp.2005.12.004

[7] Dai, Y., Sun, M., Liu, C., Li, Z. (2010). Electromagnetic wave absorbing characteristics of carbon black cement-based composites. Cement and Concrete Composites, 32(7): 508-513. https://doi.org/10.1016/j.cemconcomp.2010.03.009

[8] Wang, W.F., Xia, L.L., Xie, S. (2018). Cement-based wave absorbing material mixed with spiral carbon fiber: CN108439901A.

[9] Guo, Z.Q. (2013). Research on absorbing performance of carbon nanotube cement-based composite. Dalian University of Technology.

[10] Guo, B.W., Ding, D.H., Xiong, R. (2015). Study on electromagnetic wave absorption properties of cement-based composites mixed with natural magnetite. Functional Materials, (2): 2019-2022.

[11] He, N., Hao, W.J., Chen, W.P., Zhao, X. (2018). Research on wave absorption properties of foamed cement composites with iron tailings. New Chemical Materials, 46(10): 101-104.

[12] Nan, H.E., Hao, W., Feng, F. (2019). Electromagnetic wave absorption of iron tailings powder incorporated magnesium oxysulfate foam cement composites. Journal of Materials Science and Engineering.

[13] Dai, Y.S., Lu, C.H., Ni, Y.R., Xu, Z.Z. (2009). Research on cement-based shaped steel fiber for wave absorbing properties. Journal of Wuhan University of Technology, 31: 16-19.

[14] Dai, Y., Lu, C., Ni, Y., Xu, Z. (2009). Study on wave-absorbing properties of cement mortar with wave-shaped steel fiber. New Building Materials.

[15] He, Y., Xiao, P.H., Li, G. (2015). Preparation and microwave absorbing properties of nanometer Fe_3O_4 cement composites. Journal of Wuhan University of Technology.

[16] He, Y., Lu, L., Sun, K., Wang, F., Hu, S. (2018). Electromagnetic wave absorbing cement-based composite using Nano-Fe_3O_4 magnetic fluid as absorber. Cement and Concrete Composites, 92: 1-6. https://doi.org/10.1016/j.cemconcomp.2018.05.004

[17] Xiong, G., Deng, M., Xu, L., Tang, M. (2004). Absorbing electromagnetic wave properties of cement-based composites. Guisuanyan Xuebao(J. Chin. Ceram. Soc.)(China), 32(10): 1281-1284. https://doi.org/10.1007/BF02911033

[18] Li, B.Y., Liu, S.H. (2007). Research on absorbing performance of composite absorbent filled cement-based material. China Academic Conference on Functional Materials and Their Applications.

[19] Wu, L., Shen, G., Xu, Z., Li, R., Hu, Y. (2007). Electromagnetic wave absorbing properties of cement-based composite doped with ferrites and SiC fibers. Journal-Chinese Ceramic Society, 35(7): 904-908.

[20] Zhou, L., Wang, Z.J., Yu, J.J. (2020). Ecological cement-based composite wave absorbing material and preparation method thereof: CN111592298A.

[21] Liu, Y., Shuai, J.F., He, Z.X. (2019). Carbon fiber-carbonyl iron composite modified wave-absorbing concrete and preparation method thereof: CN110128085A.

[22] Sun, Y., Chen, M., Gao, P., Zhou, T., Liu, H., Xun, Y. (2019). Microstructure and microwave absorbing properties of reduced graphene oxide/Ni/multi-walled carbon nanotubes/Fe_3O_4 filled monolayer cement–based absorber. Advances in Mechanical Engineering, 11(1): 1687814018822886. https://doi.org/10.1177/1687814018822886

[23] Lu, B., Dong, X. L., Huang, H., Zhang, X.F., Zhu, X.G., Lei, J.P., Sun, J.P. (2008). Microwave absorption properties of the core/shell-type iron and nickel nanoparticles. Journal of Magnetism and Magnetic Materials, 320(6): 1106-1111. https://doi.org/10.1016/j.jmmm.2007.10.030

[24] Lu, L., He, Y., Ping, B., Wang, F., Hu, S. (2017). TiO_2 containing electromagnetic wave absorbing aggregate and its application in concrete. Construction and Building Materials, 134: 602-609. https://doi.org/10.1016/j.conbuildmat.2016.12.153